Research Article

Ali M. Mubaraki*

Asymptotic model for the propagation of surface waves on a rotating magnetoelastic half-space

https://doi.org/10.1515/dema-2024-0057
received April 14, 2024; accepted August 6, 2024

Abstract: This article is focused on deriving the approximate model for surface wave propagation on an elastic isotropic half-plane under the effects of the rotation and magnetic field along with the prescribed vertical and tangential face loads. The method of study depends on the slow time perturbation of the prevalent demonstration for the Rayleigh wave eigen solutions through harmonic functions. A perturbed pseudo-hyperbolic equation on the interface of the media is subsequently derived, governing the propagation of the surface wave. The established asymptotic formulation is tested by comparison with the exact secular equation. In the absence of the magnetic field, the specific value of Poisson's ratio, $\nu = 0.25$, is highlighted, where the rotational effect vanishes at the leading order.

Keywords: surface waves, magnetic field, rotational effects, secular equation, asymptotic model

MSC 2020: 74A10, 74B05, 74E10, 74F05

1 Introduction

Magnetostrictive materials are among the contemporary materials that adjust to mechanical strain when subjected to magnetic field force, in addition to their possession of magnetostrictive strains that are higher than those of piezoelectric materials. Indeed, the higher expectancy of real-world relevance of such materials has been asserted to be in so many fields, including "defence industry and aerospace, marine science and offshore engineering, machinery and automotive manufacturing, high-power ultrasound, and medical services" [1]. Mathematically, magnetoelastic coupling between the plane elastic waves and magnetic field forces via the utilization of the classical elasticity theory and Maxwell's equations opens up many interesting topics that are timely, looking at the modern advances in the present-day technological advancements. In addition, the "propagation of Rayleigh waves in a perfectly conducting elastic half-space in the presence of magnetic fields is considered for a possible application in nondestructive measurements of mechanical and/or electromagnetic parameters in electromagnetic materials" [2]. In addition, certain observational and theoretical frameworks on magneto-rotation coupling in anisotropic films were reported in the recent work of Xu et al. [3] with regard to the interaction of acoustic surface waves with ferromagnetic films, being geared by rotational deformation; moreover, the possible application of the scenario has been captured in the rectification processes, with acoustomagnetic rectifiers cited as a real example. Additionally, Li et al. [4] made use of the modified Laguerre orthogonal polynomial to examine the Rayleigh-type waves in inhomogeneous magneto-electro-elastic half-plane in relation to gigantic significance in acoustic surface wave devices; also refer [5–7] for more on the application of magnetoelastic and other modern new materials. Certainly, the surface

* **Corresponding author: Ali M. Mubaraki,** Department of Mathematics and Statistics, College of Science, Taif University, P.O. Box 11099, Taif 21944, Saudi Arabia, e-mail: alimobarki@tu.edu.sa

waves in elastic solids, such as Rayleigh waves in the Earth's crust, propagate by a combination of both longitudinal and transverse motions. Studies of surface waves in elastic solids originated from the classical contribution of Rayleigh [8]. These waves are important in many applications, such as earthquake monitoring, non-destructive testing of materials, and in the design of earthquake-resistant structures [9–11] to mention a few. However, these types of waves are confined to the surface of the solid, which makes them distinct from body waves, which propagate through the bulk of the solid. In general, surface waves travel slower than body waves, but they can cause more damage to structures due to their larger amplitudes and longer durations.

The problem related to magnetoelasticity was studied by Knopoff [12] and Chadwick [13] and further advanced by Kaliski and Petykiewicz [14]; for more on the propagation of SH waves on magnetoelastic media, refer the work of Abubakar [15]. Indeed, the problem of surface waves on a rotating magnetoelastic half-space can be formulated using asymptotic methods, through the acquisition of an approximate singularly perturbed elliptic-hyperbolic model. The starting point is to assume that the wavelength of the waves is much smaller than the characteristic length scale of the problem. This allows us to use an asymptotic expansion to derive approximate solutions for the wave motion. Besides, many researchers have laid various foundational studies with regard to the propagation of waves in dissimilar elastic media amidst the action of different body forces and other external effects. For instance, Vinh and Seriani [16] examined the propagation of surface waves on the orthotropic structures under the action of gravity; while Ting [17] analyzed the influence of the same gravity on the propagation of surface waves on general anisotropic media; read [18–23] for various submissions on wave dynamics in several elastic structures. Besides, such studies also exist in a variety of composite elastic layered media, refer to studies [24–26] that heavily utilized asymptotic approach to effectively examine the dispersion relation of layered plates under anti-plane shear assumption. The basic idea behind the asymptotic method [27] is to find an approximate solution to a problem by making easier assumptions that are valid only in the limit. This method is widely used in a variety of fields including elasticity, see [28–30] and references therein. In particular, the method is useful in situations where exact solutions are difficult or impossible to obtain, but where approximate solutions are sufficient for practical purposes.

However, the literature lacks strong revelation with regard to the propagation of surface waves on homogeneous magnetoelastic media specifically amidst the action of an external excitation, such as rotation, in addition to their quest in the design and analysis of modern materials, including magnetostrictive materials, piezoelectric materials, ferromagnetic media, multi-functional materials, electromagnetic materials, acousto-magnetic rectifiers, functionally graded piezoelectric material, and magneto-electro-elastic devices among others; hence, the present study thus attempts to derive an explicit asymptotic model for the propagation of surface waves on a homogeneous isotropic magneto-rotato elastic half-space. To derive the equations of motion for the surface waves, we begin with the equations of motion for a magnetoelastic half-space. In addition, to account for the effect of rotation, we introduce a Coriolis force term in the equations of motion [31]. Indeed, our case of rotational effect consideration is the most generalized version, in comparison with Xu et al. [3], in which only infusion rotational deformation strain in the system. Indeed, both vertical and tangential face loadings will be imposed on the face of the structure, in addition to the assumption that the structure is in a rotational frame of reference. Further, both the analytical and asymptotic approaches [18] will be deployed to examine the resulting secular equation and subsequently analyze the approximate equation of motion for surface wave propagation, of course after being acquired. Moreover, we will examine the exactness of the approximate secular equation relative to the analytical one, at the same time assess the impact of the presence of both the magnetic field intensity H_0 and the Poisson ratio ν on the propagation of the surface wave in the governing homogeneous structure. Finally, we will give some fine submissions for future consideration; indeed, for some solid foundation in this arena, one may consult [32–38], where different examinations were provided with regard to wave movements in dissimilar scenarios. In addition, one is referred to [39–41] for some recent findings on the propagation of waves in semiconductor materials. The study is organized as follows: Section 2 outlines the governing equations. Section 3 gives the formulation of the model to be tackled in the present study. Section 4 derives the secular equation analytically, while Section 5 acquires the approximate model asymptotically. Section 6 discusses the acquired approximate secular equation. Section 7 gives a particular example of interest, while Section 8 provides some concluding notes.

2 Governing equations

Let us make consideration of the generalized equation of plane motion in tensorial form, in the presence of body forces F_i for $i = 1, 2, 3$ as follows [18]:

$$\sigma_{ij,j} + F_i = \rho u_{i,tt}, \quad i = j = 1, 2, 3, \tag{1}$$

where ρ is the density of the medium; and the commas indicate differentiation with respect to corresponding variables, u_i are in-plane displacement components, while σ_{ij} are the stress components to be explicitly defined later. Additionally, when the body forces F_i are specifically considered to be due to electromagnetic field forces, then F_i admits the following explicit expression [25,37]:

$$F_i = \mu_0 H_0^2(e_{,i} - \varepsilon_0 \, \mu_0 u_{i,tt}), \quad i = j = 1, 2, 3, \tag{2}$$

where e represents the dilational expression, which is given in three-dimension as follows:

$$e = u_{1,1} + u_{2,2} + u_{3,3}, \tag{3}$$

where H_0 is the magnetic field intensity, ε_0 is the electric permeability, and μ_0 is the magnetic permeability, all induced by the magnetic field force, which is characterized by the following linearized Maxwell's equations:

$$\begin{aligned} &\mathrm{Curl}\vec{H} = \vec{J} \times \varepsilon_0 \vec{E}_{,t}, \quad \mathrm{Curl}\vec{E} = -\mu_0 \vec{H}_{,t}, \quad \mathrm{Div}\vec{H} = 0, \\ &\vec{E} = \mu_0(\vec{u}_{,t} \times \vec{H}), \quad \vec{h} = \mathrm{Curl}(\vec{u} \times \vec{H}), \quad \mathrm{Div}\vec{E} = 0, \end{aligned} \tag{4}$$

where $\vec{H} = \vec{h} + H_0$, with *vech* denoting the induced magnetic field.

In this regard, also, when the medium is presumed to be in the rotating frame, the acceleration $u_{i,tt}$ in (1) is then re-expressed in the presence of Coriolis and centripetal accelerations as follows [38]:

$$u_{i,tt} \to u_{i,tt} + 2\vec{\Omega} \times \vec{u}_{,t} + \vec{\Omega} \times (\vec{\Omega} \times \vec{u}), \tag{5}$$

where Ω represents the rotating angular velocity, while $\vec{u} = (u_1, u_2, u_3)$ and $\vec{\Omega} = (\Omega_1, \Omega_2, \Omega_3)$.

3 Formulation of the problem

To formulate the governing model, we make consideration to an isotropic magnetoelastic half-space that occupies the region $-\infty < x_1, x_2 < \infty$ and $x_3 \geq 0$, rotating about x_3-axis with the angular velocity presiding by

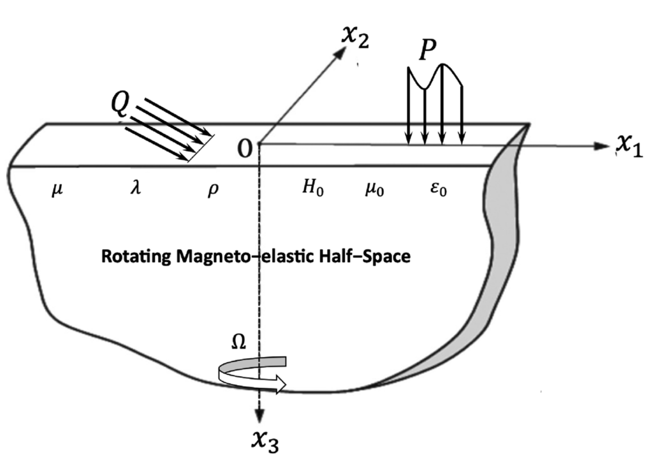

Figure 1: Rotating magneto-elastic half-space under the effects of surface loadings.

the vector $\vec{\Omega} = (0, 0, \Omega)$, along with surface loadings; comprising the vertical and tangential loads, P and Q, respectively; Figure 1 shows the schema of the structure. In fact, such consideration finds relevance in modern materials science, and in the study of turbulent and seismic waves such as earthquakes and tornados, which involve highly external excitations, alongside rotational effects.

In addition, throughout this study, we will be considering the plane strain assumption of displacement components of the following form:

$$u_1 = u_1(x_1, x_3, t) \neq 0, \quad u_2 = u_2(x_1, x_3, t) = 0, \quad u_3 = u_3(x_1, x_3, t) \neq 0, \tag{6}$$

where x_1, and x_3 are space variables, and t is the time variable. Then, the equations of motion, under the influence of rotational effects and body forces F_1 and F_3, are expressed as follows [38]:

$$\begin{aligned} \sigma_{11,1} + \sigma_{13,3} + F_1 &= \rho(u_{1,tt} - 2\Omega u_{3,t} - \Omega^2 u_1), \\ \sigma_{13,1} + \sigma_{33,3} + F_3 &= \rho(u_{3,tt} + 2\Omega u_{1,t} - \Omega^2 u_3), \end{aligned} \tag{7}$$

where ρ is the density of the medium. Additionally, $\sigma_{kl}(k, l = 1, 3)$ are the stress components defined by

$$\sigma_{kl} = \mu(u_{k,l} + u_{l,k}) + \lambda\delta_{kl}u_{k,k}, \tag{8}$$

where μ and λ are the Lame's constants; while δ_{kl} $(k, l = 1, 3)$ is the Kronecker delta function.

Here we consider the body forces F_l $(l = 1, 3)$ to be due to the magnetic field force as follows [25,37]:

$$\begin{aligned} F_1 &= \mu_0 H_0^2(u_{1,11} + u_{3,13} - \varepsilon_0\, \mu_0 u_{1,tt}), \\ F_3 &= \mu_0 H_0^2(u_{1,13} + u_{3,33} - \varepsilon_0\, \mu_0 u_{3,tt}), \end{aligned} \tag{9}$$

where the magnetic field intensity H_0, electric permeability ε_0, and magnetic permeability μ_0 are present due to the presence of the magnetic field, while Ω is the angular velocity at which the elastic medium rotates uniformly.

Therefore, on inserting (8) and (9) into (7), the equations of motion become

$$\begin{aligned} (\lambda + 2\mu + \mu_0 H_0^2)u_{1,11} + (\lambda + \mu + \mu_0 H_0^2)u_{3,13} + \mu u_{1,33} &= (\varepsilon_0\, \mu_0^2 H_0^2 + \rho)u_{1,tt} - \rho\Omega^2 u_1 + 2\rho\Omega u_{3,t}, \\ (\lambda + 2\mu + \mu_0 H_0^2)u_{3,33} + (\lambda + \mu + \mu_0 H_0^2)u_{1,13} + \mu u_{3,11} &= (\varepsilon_0\, \mu_0^2 H_0^2 + \rho)u_{3,tt} - \rho\Omega^2 u_3 - 2\rho\Omega u_{1,t}. \end{aligned} \tag{10}$$

Furthermore, the imposed boundary conditions at the surface $(x_2 = 0)$ are given by

$$\sigma_{33} + \mu_0 H_0^2(u_{1,1} + u_{3,3}) = -P, \quad \text{and} \quad \sigma_{13} = -Q, \tag{11}$$

where $Q = Q(x_1, t)$ and $P = P(x_1, t)$ are imposed tangential and vertical loads, respectively. To proceed, one adopts Lame's elastic potentials $\Phi = \Phi(x_1, x_3, t)$ and $\Psi = \Psi(x_1, x_3, t)$ in order to decompose the displacement components u_l, $(l = 1, 3)$ as follows:

$$u_1 = \Phi_{,1} - \Psi_{,3}, \quad u_3 = \Phi_{,3} + \Psi_{,1}, \tag{12}$$

upon which the coupled equations of motion (10) transform to the following:

$$\begin{aligned} \Phi_{,11} + \Phi_{,33} - \frac{1}{c_1^2}\Phi_{,tt} &= \frac{\bar{\rho}}{c_1^2}(2\Omega\Psi_{,t} - \Omega^2\Phi), \\ \Psi_{,11} + \Psi_{,33} - \frac{1}{c_2^2}\Psi_{,tt} &= -\frac{\bar{\rho}}{c_2^2}(2\Omega\Phi_{,t} + \Omega^2\Psi), \end{aligned} \tag{13}$$

along with the following transformed loaded boundary conditions at $x_2 = 0$:

$$\begin{aligned} 2\Phi_{,13} + \Psi_{,11} - \Psi_{,33} &= -\frac{Q}{\mu}, \\ (\kappa^2 - 2)\Phi_{,11} + \kappa^2\Phi_{,33} + 2\Psi_{,13} &= -\frac{P}{\mu}, \end{aligned} \tag{14}$$

with $\bar{\rho}$, c_1, c_2, and κ explicitly taking the following expressions:

$$\bar{\rho} = \frac{\rho}{\rho + \mu_0^2 H_0^2 \varepsilon_0} \quad c_1 = \sqrt{\frac{\lambda + 2\mu + H_0^2\mu_0}{\rho + \mu_0^2 H_0^2 \varepsilon_0}}, \quad c_2 = \sqrt{\frac{\mu}{\rho + \mu_0^2 H_0^2 \varepsilon_0}}, \quad \kappa = \frac{c_1}{c_2}, \tag{15}$$

where c_1 and c_2 above are the longitudinal and transverse speeds in the magnetoelastic isotropic media, respectively.

4 Secular equation

In this section, we first derive the resulting secular equation analytically by considering the loads $P = Q = 0$. In fact, the expressions for Lame's elastic potentials Φ and Ψ are harmonically presumed to take the following pattern:

$$\Phi = f(x_3)e^{ik(x_1 - ct)}, \quad \Psi = g(x_3)e^{ik(x_1 - ct)}, \quad i = \sqrt{-1}, \tag{16}$$

where k is the dimensional wave number, while c is the dimensional phase speed.

Next on inserting (16) into (13), one obtains

$$f_{,33} - k^2(\alpha^2 - \bar{\rho}\kappa^{-2}\varepsilon^2)f = -2ik^2\bar{\rho}\kappa^{-1}C_1\varepsilon g \tag{17}$$

and

$$g_{,33} - k^2(\beta^2 - \bar{\rho}\varepsilon^2)g = 2ik^2\bar{\rho}C_2\varepsilon f, \tag{18}$$

where

$$C_1 = \frac{c}{c_1}, \quad C_2 = \frac{c}{c_2}, \quad \alpha = \sqrt{1 - C_1^2}, \quad \beta = \sqrt{1 - C_2^2}, \quad \varepsilon = \frac{\Omega}{kc_2}. \tag{19}$$

It can be seen from (12) and (13) that for a specific range of wave numbers $k \gg \Omega/c_2$, or equivalently $\varepsilon \ll 1$, they become weakly coupled. This observation suggests using a perturbation approach, which will be studied later.

From equation (17), we have

$$g = \frac{i\kappa}{2k^2\bar{\rho}C_1\varepsilon}(f_{,33} - k^2(\alpha^2 - \bar{\rho}\kappa^{-2}\varepsilon^2)f). \tag{20}$$

Then, on inserting equation (20) into (18), we obtain

$$f_{,3333} - k^2\gamma_1 f_{,33} + k^4\gamma_2 f = 0, \tag{21}$$

where

$$\gamma_1 = \alpha^2 + \beta^2 - \bar{\rho}\varepsilon^2(1 + \kappa^{-2}) \quad \text{and} \quad \gamma_2 = (\alpha^2 - \bar{\rho}\kappa^{-2}\varepsilon^2)(\beta^2 - \bar{\rho}\varepsilon^2) - 4\kappa^{-1}\bar{\rho}^2C_1C_2\varepsilon^2. \tag{22}$$

The solution of (21), decaying away from the surface $x_2 = 0$, can be expressed in the form

$$f = \sum_{j=1}^{2} A_j e^{-k\lambda_j x_3}, \tag{23}$$

where $A_j, j = 1, 2$ are constants, while λ_j takes the following expression:

$$\lambda_j = \sqrt{\frac{\gamma_1 + (-1)^j\sqrt{\gamma_1^2 - 4\gamma_2}}{2}}. \tag{24}$$

Further, substituting (23) in (20), we obtain

$$g = \sum_{j=1}^{2} \chi_j A_j e^{-k\lambda_j x_3}, \tag{25}$$

where

$$\chi_j = \frac{i\kappa}{2\bar{\rho}C_1\varepsilon}(\lambda_j^2 - \alpha^2 + \bar{\rho}\kappa^{-2}\varepsilon^2). \tag{26}$$

Finally, upon inserting solutions (23) and (25) into the boundary conditions, we arrive at

$$\begin{aligned} &\sum_{j=1}^{2}[2i\lambda_j + (1 + \lambda_j^2)\chi_j]A_j = 0, \\ &\sum_{j=1}^{2}[(1 - \lambda_j^2)\kappa^2 + 2(i\chi_j\lambda_j - 1)]A_j = 0, \end{aligned} \tag{27}$$

yielding the following resulting analytical secular equation (dispersion relation):

$$\frac{2i\lambda_1 + (1 + \lambda_1^2)\chi_1}{2i\lambda_2 + (1 + \lambda_2^2)\chi_2} = \frac{(1 - \lambda_1^2)\kappa^2 + 2(i\chi_1\lambda_1 - 1)}{(1 - \lambda_2^2)\kappa^2 + 2(i\chi_2\lambda_2 - 1)}. \tag{28}$$

Hence, we graphically analyze the obtained secular equation in (28) by fixing the involving parameters as follows [25]: density $\rho = 8 \times 10^3\,\mathrm{kg\,m^{-3}}$, Young's modulus $E = 2 \times 10^2$ GPa, electric permeability $\varepsilon_0 = 8.85 \times 10^{-12}\,\mathrm{kg^{-1}m^{-3}s^4A^2}$, and the magnetic permeability $\mu_0 = 4\pi \times 10^{-7}\,\mathrm{kg\,m\,s^{-2}\,A^{-2}}$.

Figure 2 depicts the dependence of the scaled phase velocity $C_R = c/c_R$ (where c_R is the Rayleigh wave speed) on the dimensionless ε, via the exact secular relation determined (28) by varying the effects of the magnetic field intensity H_0 in Figure 2 (a) and the Poisson ratio ν in Figure 2 (b). Notably, it is vividly noted from Figure 2 that an increase in both the magnetic field intensity and the Poisson ratio increases the dependence of C_R on ε.

Furthermore, we asymptotically examine the analytically obtained exact secular equation in (28) by making consideration of the fact that $\varepsilon \ll 1$. Therefore, we expand (28) as follows:

$$D_0 + D_1\varepsilon + O(\varepsilon^2) = 0, \tag{29}$$

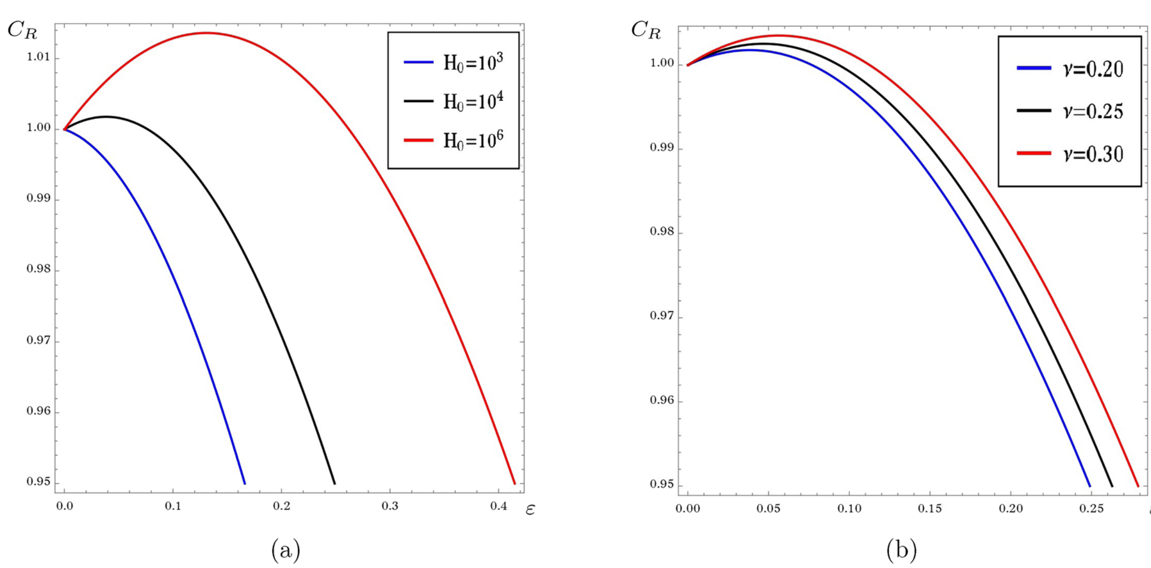

Figure 2: Relationship between the scaled phase velocity C_R and the dimensionless ε. (a) $\nu = 0.2$ and (b) $H_0 = 10^4$.

where

$$D_0 = (1+\beta^2)^2 - 4\alpha\beta,$$
$$D_1 = \frac{4\bar{\rho}}{\kappa(\alpha+\beta)}\left(\sqrt{1-\alpha^2}\,(2-\kappa^2(\alpha\beta+1)) + \sqrt{1-\beta^2}\,\kappa(1-\alpha\beta)\right). \tag{30}$$

It may be seen that the expansion in (29) contains the Rayleigh wave equation at the leading order D_0, while the effect of rotation is contained in the next order, the correction D_1.

In this regard, when $\varepsilon \gg 1$, from (19), we obtain that $k \gg \Omega c_2^{-1}$. Therefore, upon introducing the dimensionless wave number K, we obtain

$$K = \frac{c_2 k}{\Omega} \gg 1, \tag{31}$$

which is a short-wave approximation. Hence, we examine the relevance of C_R vs K via the analytically obtained exact secular relation in (28) with respect to the significance of the magnetic field intensity H_0 and the Poisson ratio ν in Figure 3 (a) and (b), respectively. Also, without much delay, it is observed that an increase in both quantities (H_0 and ν) enhances the propagation of surface waves in the magnetoelastic half-space.

5 Asymptotic model for surface waves

Here, an asymptotic model for surface waves associated with the rotating magnetoelastic half-plane under consideration is introduced below, which depends upon the approach recently deployed in [18,29].

At first, let us define the following dimensionless scaling:

$$\xi = k(x_1 - c_R t), \quad \eta = kx_3 \quad \tau = k\varepsilon c_R t. \tag{32}$$

Therefore, the transformed model in (13), coupled to the transformed conditions in (14), is then re-expressed via this new scaling as follows:

$$\Phi_{,yy} + \alpha_R^2\Phi_{,\xi\xi} + 2\varepsilon(1-\alpha_R^2)\Phi_{,\xi\tau} - \varepsilon^2(1-\alpha_R^2)\Phi_{,\tau\tau} = -\bar{\rho}\left(\frac{2(1-\alpha_R^2)}{\sqrt{1-\beta_R^2}}(\varepsilon\Psi_{,\xi} - \varepsilon^2\Psi_{,\tau}) + \kappa^{-2}\varepsilon^2\Phi\right),$$
$$\Psi_{,yy} + \beta_R^2\Psi_{,\xi\xi} + 2\varepsilon(1-\beta_R^2)\Psi_{,\xi\tau} - \varepsilon^2(1-\beta_R^2)\Psi_{,\tau\tau} = \bar{\rho}\left(2\sqrt{1-\beta_R^2}(\varepsilon\Phi_{,\xi} - \varepsilon^2\Phi_{,\tau}) - \varepsilon^2\Psi\right), \tag{33}$$

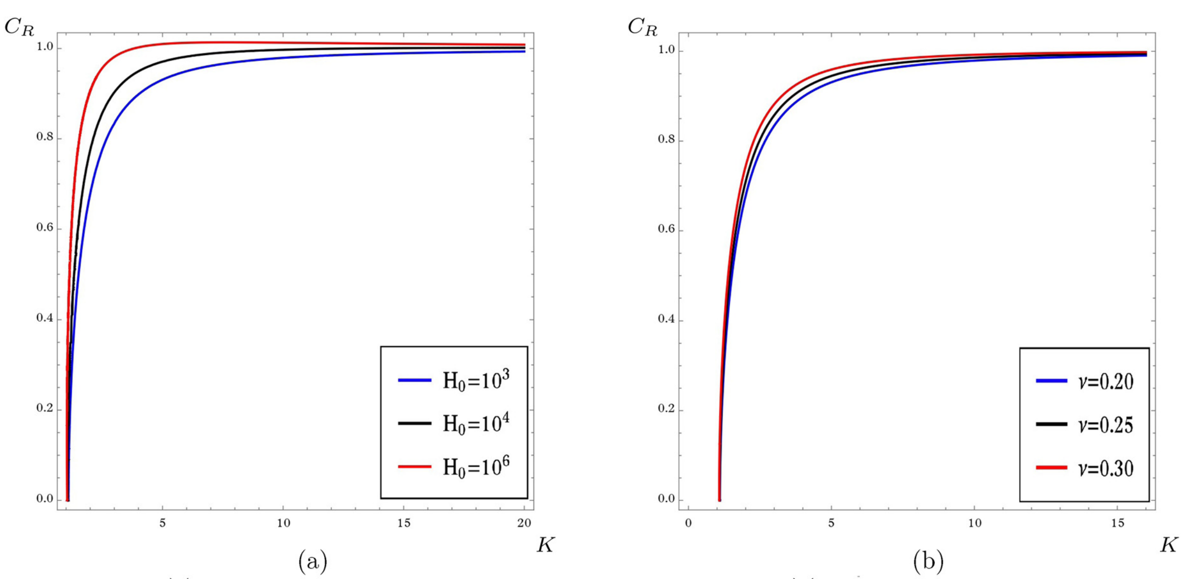

Figure 3: Relationship between the scaled phase velocity C_R and the dimensionless wave number K. (a) $\nu = 0.2$ and (b) $H_0 = 10^3$.

and

$$
\begin{aligned}
2\Phi_{,\xi\gamma} + \Psi_{,\xi\xi} - \Psi_{,\gamma\gamma} &= -\frac{Q}{k^2\mu},\\
(\kappa^2 - 2)\Phi_{,\xi\xi} + \kappa^2\Phi_{,\gamma\gamma} + 2\Psi_{,\xi\gamma} &= -\frac{P}{k^2\mu}, \quad \text{at } \gamma = 0,
\end{aligned} \tag{34}
$$

where

$$
\alpha_R = \sqrt{1 - \frac{c_R^2}{c_1^2}}, \quad \text{and} \quad \beta_R = \sqrt{1 - \frac{c_R^2}{c_2^2}}. \tag{35}
$$

Now, we make use of an asymptotic series to expand the Lamé elastic potentials Φ and Ψ as a series of terms, where each term corresponds to a different order in the small parameter ε as follows:

$$
\begin{aligned}
\Phi &= \varepsilon^{-1}(\Phi_0(\xi, \gamma, \tau) + \varepsilon\Phi_1(\xi, \gamma, \tau) + \ldots),\\
\Psi &= \varepsilon^{-1}(\Psi_0(\xi, \gamma, \tau) + \varepsilon\Psi_1(\xi, \gamma, \tau) + \ldots),
\end{aligned} \tag{36}
$$

such that at leading order (ε^{-1}), equation (33) and the boundary equation (34) become

$$
\Phi_{0,\gamma\gamma} + \alpha_R^2\Phi_{0,\xi\xi} = 0, \quad \Psi_{0,\gamma\gamma} + \beta_R^2\Psi_{0,\xi\xi} = 0, \tag{37}
$$

and

$$
\begin{aligned}
2\Phi_{0,\xi\gamma} + \Psi_{0,\xi\xi} - \Psi_{0,\gamma\gamma} &= 0,\\
(\kappa^2 - 2)\Phi_{0,\xi\xi} + \kappa^2\Phi_{0,\gamma\gamma} + 2\Psi_{0,\xi\gamma} &= 0, \quad \text{at } \gamma = 0.
\end{aligned} \tag{38}
$$

Thus, equation (37) admits the following solutions:

$$
\Phi_0 = \Phi_0(\xi, \alpha_R\gamma, \tau), \quad \text{and} \quad \Psi_0 = \Psi_0(\xi, \beta_R\gamma, \tau). \tag{39}
$$

Next on inserting the harmonic solutions (39) into the boundary conditions expressed in (38), and thereafter, upon using the characteristics of harmonic functions, we obtain

$$
\begin{aligned}
2\alpha_R\Phi_{0,\xi\xi} + (1 + \beta_R^2)\mathcal{H}(\Psi_{0,\xi\xi}) &= 0,\\
(1 + \beta_R^2)\Phi_{0,\xi\xi} + 2\beta_R\mathcal{H}(\Psi_{0,\xi\xi}) &= 0, \quad \text{at } \gamma = 0,
\end{aligned} \tag{40}
$$

where $\mathcal{H}$ denotes the Hilbert transform.

Indeed, the famous secular equation by the name “Rayleigh equation” is obtained from (40) as follows:

$$
(1 + \beta_R^2)^2 - 4\alpha_R\beta_R = 0, \tag{41}
$$

along with

$$
\mathcal{H}(\Psi_0) = -\lambda\Phi_0 \quad \text{and} \quad \Psi_0 = \lambda\mathcal{H}(\Phi_0), \tag{42}
$$

where

$$
\lambda = \frac{2\alpha_R}{1 + \beta_R^2} = \frac{1 + \beta_R^2}{2\beta_R}. \tag{43}
$$

From equation (33), we obtain the next order

$$
\begin{aligned}
\Phi_{1,\gamma\gamma} + \alpha_R^2\Phi_{1,\xi\xi} &= -2(1 - \alpha_R^2)\Phi_{0,\xi\tau} - \frac{2\bar{\rho}(1 - \alpha_R^2)}{\sqrt{1 - \beta_R^2}}(\Psi_{0,\xi}),\\
\Psi_{1,\gamma\gamma} + \beta_R^2\Psi_{1,\xi\xi} &= -2(1 - \beta_R^2)\Psi_{0,\xi\tau} + 2\bar{\rho}\sqrt{1 - \beta_R^2}(\Phi_{0,\xi}).
\end{aligned} \tag{44}
$$

Corrector terms Φ_1 and Ψ_1 may be represented by

$$\Phi_1 = \varphi_1 + y\varphi_2 + \varphi_3 \quad \text{and} \quad \Psi_1 = \psi_1 + y\psi_2 + \psi_3, \tag{45}$$

where $\varphi_j = \varphi_j(\xi, \alpha_R y, \tau)$ and $\psi_j = \psi_j(\xi, \beta_R y, \tau)$, $j = 1, 2$ are arbitrary plane harmonic functions. Consequently, with regard to the harmonic functions φ_2 and ψ_2, we obtain

$$\varphi_2 = -\frac{(1-\alpha_R^2)}{\alpha_R}\mathcal{H}(\Phi_{0,\tau}), \quad \text{and} \quad \psi_2 = -\frac{(1-\beta_R^2)}{2\beta_R}\mathcal{H}(\Psi_{0,\tau}), \tag{46}$$

whereas for the particular solutions $\varphi_3 = \varphi_3(\xi, \beta_R y, \tau)$ and $\psi_3 = \psi_3(\xi, \alpha_R y, \tau)$, we obtain

$$\varphi_{3,\xi} = \frac{2\bar{\rho}(1-\alpha_R^2)}{(\beta_R^2-\alpha_R^2)\sqrt{1-\beta_R^2}}\Psi_0, \quad \text{and} \quad \psi_{3,\xi} = \frac{2\bar{\rho}\sqrt{1-\beta_R^2}}{\beta_R^2-\alpha_R^2}\Phi_0. \tag{47}$$

At next order, the boundary conditions (34) at $y = 0$ become

$$\begin{aligned} 2\Phi_{1,\xi y} + \Psi_{1,\xi\xi} - \Psi_{1,yy} &= -\frac{Q}{k^2\mu}, \\ (\kappa^2-2)\Phi_{1,\xi\xi} + \kappa^2\Phi_{1,yy} + 2\Psi_{1,\xi y} &= -\frac{P}{k^2\mu}. \end{aligned} \tag{48}$$

Employing (45), (46), and (47), we infer at $y = 0$

$$\begin{aligned} &2\alpha_R\varphi_{1,\xi\xi} + (1+\beta_R^2)\mathcal{H}(\psi_{1,\xi\xi}) + 2\left(\frac{1-\alpha_R^2}{\alpha_R} - \frac{2(1-\beta_R^2)\alpha_R}{1+\beta_R^2}\right)\Phi_{0,\xi\tau} \\ &\quad + \frac{2\bar{\rho}}{(\beta_R^2-\alpha_R^2)\sqrt{1-\beta_R^2}}[(1-\alpha_R^2)(1+\beta_R^2) + (1+\alpha_R^2)(1-\beta_R^2)]\mathcal{H}(\Phi_{0,\xi}) = -\frac{\mathcal{H}(Q)}{k^2\mu} \\ &-(1+\beta_R^2)\varphi_{1,\xi\xi} - 2\beta_R\mathcal{H}(\psi_{1,\xi\xi}) + 2\left(\frac{2\alpha_R}{(1+\beta_R^2)\beta_R} - 1\right)\Phi_{0,\xi\tau} \\ &\quad + \frac{4\bar{\rho}\alpha_R}{(\beta_R^2-\alpha_R^2)\sqrt{1-\beta_R^2}(1+\beta_R^2)}[(\kappa^2(1-\beta_R^2)-2)(1-\alpha_R^2) - (1-\beta_R^4)]\mathcal{H}(\Phi_{0,\xi}) = -\frac{P}{k^2\mu}. \end{aligned} \tag{49}$$

Then, the solvability of (49) gives at $y = 0$

$$2\Phi_{0,\xi\tau} + B_R\mathcal{H}(\Phi_{0,\xi}) = -\frac{1}{2k^2\mu B}[(1+\beta_R^2)P + 2\beta_R\mathcal{H}(Q)], \tag{50}$$

where

$$B_R = \frac{4\bar{\rho}}{B(\beta_R^2-\alpha_R^2)\sqrt{1-\beta_R^2}}\left[\beta_R(1-\alpha_R^2\beta_R^2) + \frac{1}{2}\alpha_R((\kappa^2(1-\beta_R^2)-2)(1-\alpha_R^2) - (1-\beta_R^4))\right], \tag{51}$$

with

$$B = (1-\alpha_R^2)\frac{\beta_R}{\alpha_R} + (1-\beta_R^2)\frac{\alpha_R}{\beta_R} - (1-\beta_R^4). \tag{52}$$

Additionally, upon utilizing the leading order approximation, we obtain

$$\Phi \approx \frac{1}{\varepsilon}\Phi_0, \quad \Psi \approx \frac{1}{\varepsilon}\Psi_0, \tag{53}$$

along with operator identities

$$2\varepsilon\partial_{\xi\tau} = \frac{1}{k^2}\left(\partial_{11} - \frac{1}{c_R^2}\partial_{tt}\right) + O(\varepsilon^2), \tag{54}$$

then (50) can be expressed using the original dimensional variables (x_1, x_2, t) at the surface $x_2 = 0$, that is,

$$\Phi_{,11} - \frac{1}{c_R^2}\Phi_{,tt} + \frac{\Omega B_R}{c_2}\mathcal{H}(\Phi_{,1}) = -\frac{1}{2\mu B}[(1 + \beta_R^2)P + 2\beta_R\mathcal{H}(Q)]. \tag{55}$$

In addition, the equation representations for the potentials functions Φ and Ψ are obtained using the following elliptic equations from equations (33) as:

$$\Phi_{,33} + \alpha_R^2\Phi_{,11} = 0, \quad \text{and} \quad \Psi_{,33} + \beta_R^2\Psi_{,11} = 0, \tag{56}$$

while the relationship between the two potential functions at the surface is found to be

$$\Psi_{,1}(x_1, 0, t) = -\frac{2}{1 + \beta_R^2}\Psi_{,2}(x_1, 0, t), \tag{57}$$

following from (42).

6 Discussion of the approximate secular equation

Proceeding, equation (55) could be written using the related pseudo-differential operator at $x_2 = 0$ as follows:

$$\Phi_{,11} - \frac{1}{c_R^2}\Phi_{,tt} + \frac{\Omega B_R}{c_2}\sqrt{-\partial_{11}}\,\Phi = -\frac{1}{2\mu B}[(1 + \beta_R^2)P + 2\beta_R\mathcal{H}(Q)]. \tag{58}$$

In particular, the later boundary equation coincides with [18] in case of no rotation; see also [28] for a similar situation but without the action of the magnetic field force.

Consequently, we can deduce from (58) the approximation of the secular equation under the combined effects of rotation and magnetic field in the absence of effective loading ($P = Q = 0$) as follows:

$$C_R = \sqrt{1 - \frac{\Omega B_R}{kc_2}}, \tag{59}$$

where the above equation may equally be expressed in terms of ε in $(19)_4$ as

$$C_R = \sqrt{1 - \varepsilon B_R}, \tag{60}$$

or through the dimensionless wave number K in (31) as

$$C_R = \sqrt{1 - \frac{B_R}{K}}. \tag{61}$$

The coefficient B_R represents the influence of rotation on the propagation of surface waves at a leading order. The approximation outlined in (61) takes into consideration the sign of the coefficient B_R defined by equation (51), which is contingent upon Poisson's ratio ν (Figure 4). Here, and in the following discussion, we employ the magnetoelastic properties [25]: $\mu_0 = 4\pi \times 10^{-7}\,\mathrm{kg\,m\,s^{-2}A^{-2}}$, and $\varepsilon_0 = 8.85 \times 10^{-12}\,\mathrm{kg^{-1}\,m^{-3}s^4A^2}$, along with $E = 2 \times 10^2$ GPa, and $\rho = 8 \times 10^3\,\mathrm{kg\,m^{-3}}$.

From Figure 1, it can be noted that the constant B_R is positive when $0 < \nu < 0.25$, $0 < \nu < 0.24$, and $0 < \nu < 0.22$ and negative when $0.25 < \nu < 0.5$, $0.24 < \nu < 0.5$, and $0.22 < \nu < 0.5$ for $H_0 = 0$, $H_0 = 2{,}000$, and $H_0 = 3{,}000$, respectively. Additionally, it is observed that in cases of $H_0 = 0$, $H_0 = 2{,}000$, and $H_0 = 3{,}000$, the constant $B_R = 0$ at Poisson's ratio $\nu = 0.25$, $\nu = 0.24$, and $\nu = 0.22$, respectively. Under this circumstance, equation (58) simplifies to the established hyperbolic-elliptic model for Rayleigh waves in [27]. In addition, graphical comparison between the analytically obtained exact secular equation in (28) and those of the asymptotic relations (60) and (61) are depicted in Figure 5, showing the relationships between the dimensionless phase speed C_R against the dimensionless ε and the wave number K, respectively. In addition, in the same Figure 5, the solid and dashed lines indicate the exact dispersion relation in equation (28) and the approximation in equation (60) or (61), respectively.

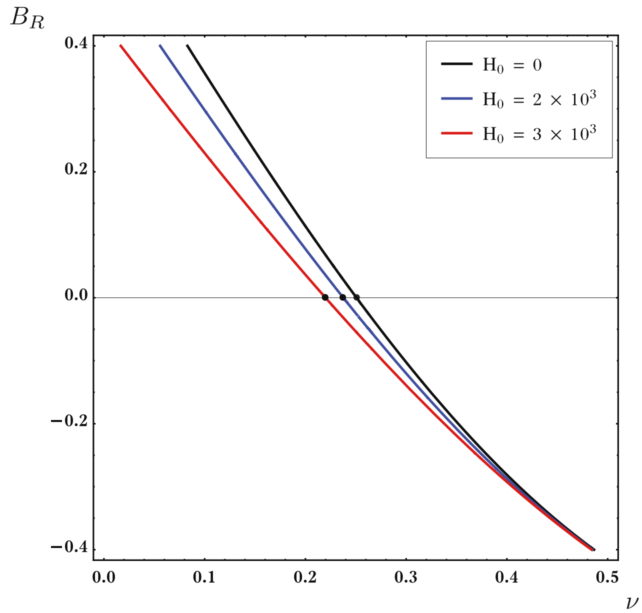

Figure 4: Relationship between B_R in equation (44) against the Poisson's ratio ν.

Hence, as Figure 5 (a) illustratively depicts the comparison between the exact and approximate secular equations by portraying the relationship between C_R vs ε for several fixed values of H_0, it is therefore noted that the disparity between the two equations shrinks with an increase in H_0; in fact, there is a mounting hope that the two would be equal upon suitably choosing an appropriate value for the magnetic field intensity H_0. However, an opposite trend is noted in Figure 5 (b), with regard to the relationship between C_R vs K; in fact, an agreement is attained between the two secular equations when H_0 is chosen relatively smaller than 10^3. Besides, one would clearly see the depictions of the harmonic curves when H_0 takes the values 10^4 and 10^6, sequentially, where partial-sided conformity is achieved on the K axis, which is a kind of short-wave propagation. Note that the overall development depends on the sign for the coefficient B_R, that is, whether positive or negative.

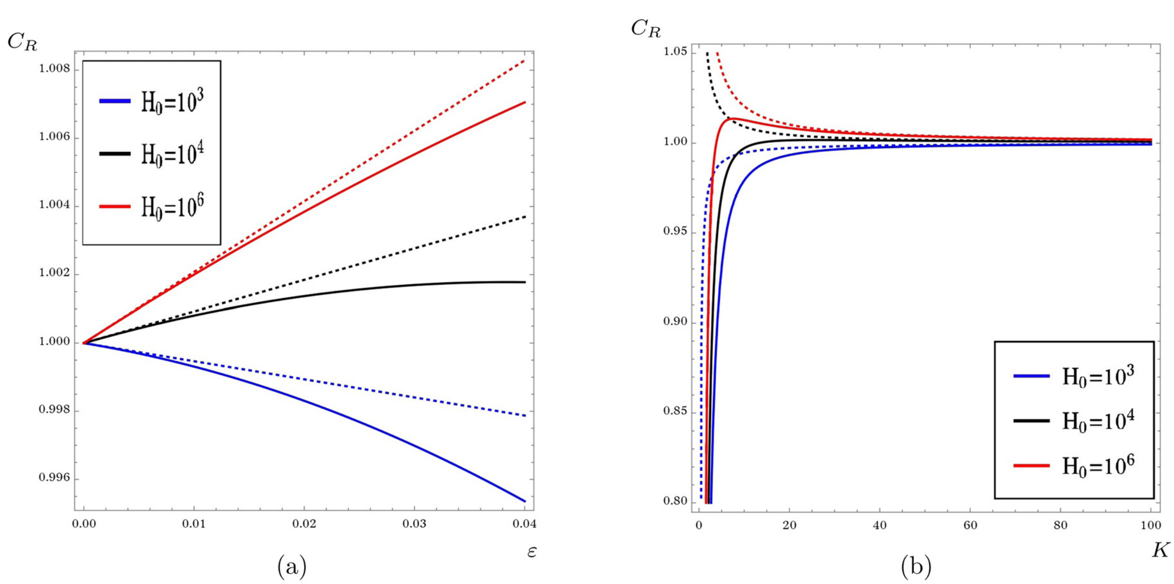

Figure 5: Comparison between the exact (solid line) and the leading asymptotic (dashed line) secular equations (a) C_R versus epsilon (b) C_R versus K.

7 Example: moving point load

In this example, we simulate near-resonant regimes of the moving point of vertical stress P only, to demonstrate the effectiveness of the proposed approximate formulations for the Rayleigh wave. As might be expected, the dynamic response caused by a load travels at a speed close to the Rayleigh wave speed. For the present governing problem, the suggested model for the surface wave includes an elliptic equation for the interior $x_3 > 0$, given as in (56), along with boundaries (57) at $x_3 = 0$. Now, let us rewrite the boundary value problem expressed in (56) and (58) in the moving coordinate system $(r, x_3) = (x_1 - ct, x_3)$. Hence, the steady state limit is governed by

$$\Phi_{,33} + \alpha_R^2 \Phi_{,rr} = 0, \tag{62}$$

and associated by the boundary condition at $x_3 = 0$ as follows:

$$\Gamma \Phi_{,rr} + \frac{\Omega B_R}{c_2} \sqrt{-\partial_{rr}}\, \Phi = -\frac{(1 + \beta_R^2)}{2\mu B} P_0 \delta(r), \tag{63}$$

where the vertical applied load P is considered in the form of Delta function, P_0 is a constant, and $|\Gamma| = |1 - C_R| \ll 1$ corresponds to the near-resonant region.

In addition, let us take

$$r = \left| \frac{\Gamma}{B_R} \right| \frac{c_2}{\Omega} \zeta, \quad \text{and} \quad \Theta = -\frac{2\mu B \Omega B_R}{P_0 c_2 (1 + \beta_R^2)} \Phi, \tag{64}$$

then equation (63) is rewritten as

$$\operatorname{sign}(\Gamma B_R) \Theta_{,\zeta\zeta} + \sqrt{-\partial_{\zeta\zeta}}\, \Theta = \delta(\zeta). \tag{65}$$

The solution of the latter equation is then obtained through the application of the Fourier integral transform as follows:

$$\Theta = \frac{1}{2\pi} \int_{-\infty}^{\infty} \frac{e^{i\omega\zeta} \mathrm{d}\omega}{\omega(1 - \operatorname{sign}(\Gamma B_R)\omega)} = \frac{1}{\pi} \lim_{a \to 0} \operatorname{Re} \int_{a}^{\infty} \frac{\cos(\omega\zeta)}{\omega(1 - \operatorname{sign}(\Gamma B_R)\omega)} \mathrm{d}\omega. \tag{66}$$

Here we restrict ourselves only to the case of no poles on the real axis with $\omega > 0$ and $\operatorname{sign}(\Gamma B_R) < 0$, then the integral (66) gives the solution

$$\Theta = \frac{1}{\pi} \left[\cos(|\zeta|) \operatorname{Ci}((a + 1)|\zeta|) - \operatorname{Ci}(a|\zeta|) - \frac{1}{2} \sin(|\zeta|)(\pi - 2 \operatorname{Si}((a + 1)|\zeta|)) \right], \quad a \sim 0. \tag{67}$$

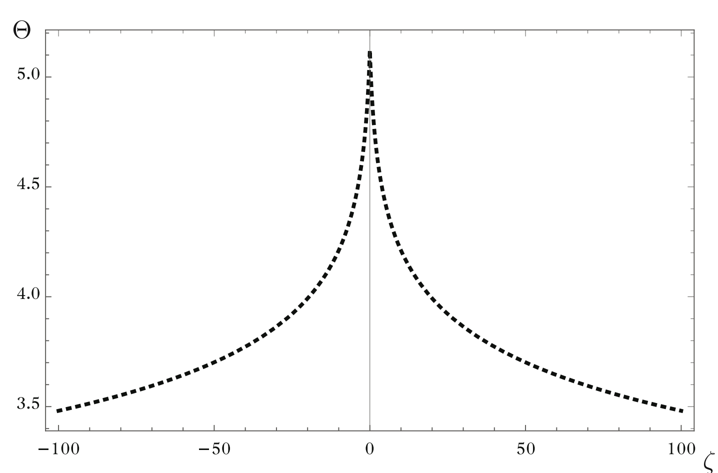

Figure 6: Relationship between the quantity Θ and the moving coordinate ζ.

where

$$\mathrm{Ci}(y) = -\int_{y}^{\infty} \frac{\cos y}{y} \mathrm{d}t, \quad \text{and} \quad \mathrm{Si}(y) = -\int_{y}^{\infty} \frac{\sin y}{y} \mathrm{d}t, \tag{68}$$

see e.g. [42]. Note that this scenario can occur either in the sub-critical regime ($C_R < 1$) with a sign of the coefficient $B_R < 0$ or in the super-Rayleigh regime ($C_R > 1$) with $B_R > 0$.

Moreover, this scenario has been captured in Figure 6, showing the variational effect of the quantity Θ on the moving coordinate ζ when $a = 10^{-9}$. Indeed, the steady-state problem for moving point load on a rotating elastic half-plane is illustrated in the figure, using the approximate model for the Rayleigh wave, which gives an explicit near-resonant solution.

8 Conclusion

In conclusion, an explicit model of the Rayleigh waves in a homogeneous isotropic magnetoelastic half-space has been derived, with the structure framed under rotational reference. Generalized mechanical vertical and tangential excitation loads are further incorporated into the surface of the structure. Analytical and asymptotic approaches were first deployed for the analysis of the resulting secular equation and thereafter, concentrated hugely on the derivation and analysis of the approximate equation of motion for surface wave propagation. Notably, it was observed that an increase in both H_0 and ν enhanced the propagation of surface waves in the media. Further, it is noted that the disparity between the exact and approximate secular equations shrinks with an increase in H_0; in fact, there is a mounting hope that the two would be equal upon suitably choosing an appropriate value for the magnetic field intensity H_0. It was also verified that when considering Poisson's ratio, such as when $\nu = 0.25$ at leading order, the influence of rotation disappears when there is no magnetic field present. This aspect holds significance for numerous applications within the field of electrical engineering.

In this regard, further developments can include analysis of a second-order refined model [22], the 3D moving load problem [23], and the generalization to the case of anisotropy [43] by incorporating magnetic field force and rotation; indeed, a scenario of material inhomogeneity could equally be an interesting future prospect. Finally, the asymptotic formulation provides a useful tool for analyzing the behavior of surface waves on a rotating magnetoelastic half-space. The resulting equations can be used to gain insights into complex models of such nature and to design several experiments to study wave motion in more detail. Besides, it is hopeful that the renowned Lie's symmetry method [44,45], which gives multiple invariant solutions for wave equations (in particular), will be utilized to project and the propagating wave in the media. Indeed, the present study will find relevance in modern materials science, and in the study of turbulent and seismic waves such as earthquakes and tornados, which involve highly external excitations, alongside rotational effects. In addition, the study is expected to play a vital part in the production of earthquake-resisting structures, in addition to its relevance in new materials like magnetostrictive materials, ferromagnetic films, multi-functional materials, electromagnetic materials, acoustomagnetic rectifiers, and magneto-electro-elastic devices among others.

Acknowledgements: The author extends his appreciation to Taif University, Saudi Arabia, for supporting this work through project number (TU-DSPP-2024-231).

Funding information: This research was funded by Taif University, Taif, Saudi Arabia (TU-DSPP-2024-231).

Author contributions: A.M. Mubaraki: conceptualization, methodology, software, validation, formal analysis, investigation, resources, writing – original draft, writing – review and editing, visualization, supervision, and project administration.

Conflict of interest: The author declares that he has no conflicts of interest associated with this work.

References

[1] Z. Liu and H. Qi, *Dynamic anti-plane behavior of rare earth giant magnetostrictive medium with a circular cavity defect in semi-space*, Sci. Rep. **11** (2021), 13442.

[2] J. S. Lee and E. N. Its, *Propagation of Rayleigh waves in magneto-elastic media*, J Appl Mech. **59** (1992), no. 4, 812–818.

[3] M. Xu, K. Yamamoto, J. Puebla, K. Baumgaertl, B. Rana, K. Miura, et al., *Nonreciprocal surface acoustic wave propagation via magneto-rotation coupling*, Sci. Adv. **6** (2020), no. 32, eabb1724, DOI: https://doi.org/10.1126/sciadv.abb1724.

[4] K. Li, S. Jing, J. Yu, and B. Zhang, *Complex Rayleigh waves in nonhomogeneous magneto-electro-elastic half-spaces*, Materials **14** (2021), 1011, DOI: https://doi.org/10.3390/ma14041011.

[5] H. Y. Kuo and K. C. Hsin, *Functionally graded piezoelectric-piezomagnetic fibrous composites*, Acta Mech. **229** (2018), 1503–1516.

[6] J. Qiu, J. Tani, T. Ueno, T. Morita, H. Takahashi, and H. Du, *Fabrication and high durability of functionally graded piezoelectric bending actuators*, Smart Mater. Struct. **12** (2003), 115–121.

[7] R. Tian, J. Liu, and X. Liu, *Magnetoelectric properties of piezoelectric-piezomagnetic composites with elliptical nanofibers*, Acta Mech. Solida Sin. **33** (2020), 368–380.

[8] L. Rayleigh, *On waves propagated along the plane surface of an elastic solid*, Proc. Lond. Math. Soc. **1** (1885), no. 1, 4–11.

[9] A. Palermo, S. Krodel, A. Marzani, and C. Daraio, *Engineered metabarrier as shield from seismic surface waves*, Sci. Rep. **6** (2016), no. 1, 1–10.

[10] Y. S. Cho, *Non-destructive testing of high strength concrete using spectral analysis of surface waves*, NDT & E Int. **36** (2003), no. 4, 229–35.

[11] V. V. Krylov, *Noise and vibration from high-speed trains*, Thomas Telford, London, 2001.

[12] L. Knopoff, *The interaction between elastic wave motions and magnetic field in electrical conductors*, J. Geophys. Res. **60** (1955), no. 4, 441–456.

[13] P. Chadwick, *Elastic wave propagation in a magnetic field*, Aces IX Congr. Int. Mech. Appl. **7** (1957), 143–158.

[14] S. Kaliski and J. Petykiewicz, *Equation of motion coupled with the field of temperature in a magnetic field involving mechanical and electrical relaxation for anisotropic bodies*. Proc. Vib. Probl. **2** (1959), no. 17.

[15] I. Abubakar, *Magneto-elastic SH-type of motion*, Pure Appl. Geophys. **59** (1964), 10–20.

[16] P. C. Vinh and G. Seriani, *Explicit secular equations of Rayleigh waves in a non-homogeneous orthotropic elastic medium under the influence of gravity*, Wave Motion **46** (2009), no. 7, 427–434.

[17] T. C. T. Ting, *Surface waves in an exponentially graded, general anisotropic elastic material under the influence of gravity*, Wave Motion **48** (2011), no. 4, 335–344.

[18] A. M. Mubaraki and F. M. Almalki, *Surface waves on a coated homogeneous half-space under the effects of external forces*, Symmetry **14** (2022), no. 11, 2241.

[19] D. M. Barnett and J. Lothe, *Consideration of the existence of surface wave (Rayleigh wave) solutions in anisotropic elastic crystals*, J. Phys. F: Metal Phys. **4** (1974), no. 5, 671.

[20] Y. B. Fu and A. Mielke, *A new identity for the surface-impedance matrix and its application to the determination of surface-wave speeds*. Proc. R. Soc. Lond. A: Math. Phys. Eng. Sci. **458** (2002), no. 2026, 2523–2543.

[21] S. Nath and P. R. Sengupta, *Influence of gravity on propagation of waves in a medium in presence of a compressional source*. Sadhana **24** (1999), no. 6, 495–505.

[22] P. T. Wootton, J. Kaplunov, and D. Prikazchikov, *A second-order asymptotic model for Rayleigh waves on a linearly elastic half plane*, IMA J. Appl. Math. **85** (2020), no. 1, 113–131.

[23] J. Kaplunov, D. A. Prikazchikov, B. Erbaš, and O. Šahin, *On a 3D moving load problem for an elastic half space*, Wave Motion **50** (2013), no. 8, 1229–1238.

[24] R. I. Nuruddeen, R. Nawaz, and Z. Q. M. Zia, *Asymptotic analysis of an anti-plane shear dispersion of an elastic five-layered structure amidst contrasting properties*. Arch. Appl. Mech. **90** (2020), 1875–1892.

[25] R. INuruddeen, R. Nawaz, and Z. Q. M. Zia, *Effects of thermal stress, magnetic field and rotation on the dispersion of elastic waves in an inhomogeneous five-layered plate with alternating components*. Sci. Prog. **103** (2020), 0036850420940469.

[26] M. Asif, R. I. Nuruddeen, and R. Nawaz, *Propagation of elastic waves in a magneto-elastic layer laying over a light Winkler foundation with rotation*, Waves Random Complex Media, 2023. DOI: https://doi.org/10.1080/17455030.2023.2171502.

[27] J. Kaplunov and D. A. Prikazchikov, *Asymptotic theory for Rayleigh and Rayleigh-type waves*, Adv. Appl. Mech. **50** (2017), 1–106.

[28] J. Kaplunov, A. Zakharov, and D. Prikazchikov, *Explicit models for elastic and piezoelastic surface waves*. IMA J. Appl. Math. **71** (2016), no. 5, 768–782.

[29] H. H. Dai, J. Kaplunov, and D. A. Prikazchikov, *A long-wave model for the surface elastic wave in a coated half-space*, Proc. R. Soc. A: Math. Phys. Eng. Sci. **466** (2010), no. 2122, 3097–3116.

[30] N. Ege, B. Erbasss, and D. A. Prikazchikov, *On the 3D Rayleigh wave field on an elastic half-space subject to tangential surface loads*, ZAMM - J. Appl. Math. Mech. **95** (2015), no. 12, 1558–1565.

[31] S. M. Abo-Dahab, A. M. Abd-Alla, and A. Khan, *Rotational effect on Rayleigh, Love and Stoneley waves in non-homogeneous fibre-reinforced anisotropic general viscoelastic media of higher order*, Struct. Eng. Mech. **58** (2016), 181–197.

[32] M. Destrade, *Seismic Rayleigh waves on an exponentially graded, orthotropic half-space*, Proc. R. Soc. A: Math. Phys. Eng. Sci. **463** (2007), no. 2078, 495–502.

[33] P. Chadwick, *Surface and interfacial waves of arbitrary form in isotropic elastic media*, J. Elast. **6** (1976), no. 1, 73–80.

[34] F. G. Friedlander, *On the total reflection of plane waves*, Quart. J. Mech. Appl. Math. **1** (1948), no. 1, 376–384.

[35] S. L. Sobolev, P. Frank, and R. von Mises, *Some problems in wave propagation*, Diff. Integ. Equ. Math. Phys. (1937), 468–617.

[36] A. P. Kiselev and D. F. Parker, *Omni-directional Rayleigh, Stoneley and Schölte waves with general time dependence*, Proc. R. Soc. A: Math. Phys. Eng. Sci. **466** (2010), 2241–2258.

[37] A. Mubaraki, S. Althobaiti, and R. I. Nuruddeen, *Propagation of surface waves in a rotating coated viscoelastic half-space under the influence of magnetic field and gravitational forces*, Fractal Fract. **5** (2021), 1–16.

[38] M. Schoenberg and D. Censor, *Elastic waves in rotating media*, Quarter. Appl. Math. **31** (1973), 115–125.

[39] A. M. SMahdy, K. Lotfy, A. A. EL-Bary, and H. H. Sarhan, *Effect of rotation and magnetic field on a numerical-refined heat conduction in a semiconductor medium during photo-excitation processes*, Eur. Phys. J. Plus, **136** (2021), 553.

[40] A. M. S. Mahdy, K. Lotfy, A. A. EL-Bary, and I. M. Tayel, *Variable thermal conductivity and hyperbolic two-temperature theory during magneto-photothermal theory of semiconductor induced by laser pulses*, Eur. Phys. J. Plus **136** (2021), 651.

[41] M. Yasein, N. Mabrouk, K. Lotfy, and A. A. EL-Bary, *The influence of variable thermal conductivity of semiconductor elastic medium during photothermal excitation subjected to thermal ramp type*, Results Phys. **25** (2019), no. 12, 4731–4740.

[42] M. Abramowitz and I. A. Stegun, *Handbook of Mathematical Functions with Formulas, Graphs, and Mathematical Tables*, vol. 55, US Government Printing Office, 1968.

[43] Y. Fu, J. Kaplunov, and D. Prikazchikov, *Reduced model for the surface dynamics of a generally anisotropic elastic half-space*, Proc. R. Soc. A **476** (2020), no. 2234, p. 20190590.

[44] S. Shagolshem, B. Bira, and D. Zeidan, *Study of wave propagation in arterial blood flow under symmetry analysis*, Math. Methods Appl. Sci. **46** (2023), no. 4, 3522–3533.

[45] T.-T. Zhang, *On Lie symmetry analysis, conservation laws and solitary waves to a longitudinal wave motion equation*, Appl. Math. Lett. **98** (2019), 199–205.